The Metal Promoted Hydration of Di-2-pyridyl Ketone: UV–Vis Spectra of Cu(II) and Cr(III) in Aqueous Solution with Di-2-Pyridyl Ketone and the X-ray Structure Analysis of Bis-2,2′,*N*,*N*′-bipyridyl Ketone Hydrate Chromium(III) Chloride and Ruthenium

SHAUN SOMMERER, WILLIAM P. JENSEN*

Department of Chemistry, South Dakota State University, Brookings, SD 57007 (U.S.A.)

and ROBERT A. JACOBSON

Ames Laboratory, USDOE and Department of Chemistry, Iowa State University, Ames, IA 50011 (U.S.A.)

(Received July 6, 1989)

Abstract

The crystal structures of the bipyridyl ketone hydrate complexes **I**, $CrC_{22}H_{26}N_4O_8Cl$ and **II**, $RuC_{22}H_{34}N_4O_{12}$ have been determined by X-ray methods. Crystal data are: **I**, monoclinic space group $C2/c$, $Z = 4$, $a = 11.19(1)$, $b = 14.67(1)$, $c = 17.12(1)$ Å, $\beta = 104.06(1)°$; **II**, triclinic space group $P\bar{1}$, $Z = 1$, $a = 9.829(9)$, $b = 8.829(9)$, $c = 8.908(7)$ Å, $\alpha = 99.79(6)$, $\beta = 103.04(6)$, $\gamma = 76.30(7)°$. In both cases hydration occurs across the ketone double bond in the ligand and one of the hydrate oxygen atoms bonds to the metal to form a tridentate chelate. UV–Vis spectra of solutions of Cu(II) and Cr(III) with bipyridyl ketone, BPK, reveal that initial coordination of BPK and the metal is rapid but that weeks are required to form the complex compounds that crystallize from solution. The absorption spectra are shown to be pH dependent. The metal to ligand bond distances are **I**, Cr–O 1.939(5), Cr–N 2.061(5), 2.055(6) Å; **II**, Ru–O 1.975(4), Ru–N 2.057(4), 2.065(5) Å.

An approximate correlation between off-axis angles of the coordinated oxygen atoms and the difference between square planar and octahedral crystal field stabilization energy in ten reported BPK hydrate complexes is indicated.

Introduction

The metal promoted hydration of di-2-pyridyl ketone (DPK) has been of interest for some time since the ligand has the ability to undergo a reaction after initial coordination to a transition metal ion. DPK also has the ability to coordinate initially via one of two modes, either through the two nitrogen atoms of the pyridine rings or through one nitrogen atom and the carbonyl group of the ligand. At present evidence shows that in aqueous solution the former mode is favored. The observed reaction is hydration of the carbonyl forming a diol group as can be seen in Fig. 1.

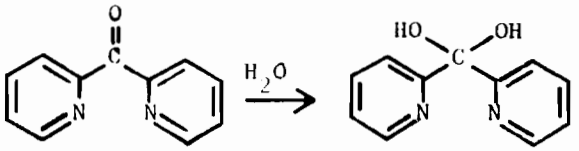

Fig. 1. DPK and DPK hydrate.

The hydration of the ketone is interesting since it is well known that ketones do not normally hydrate to any significant extent unless they are flanked on either side by very strong electron-withdrawing groups. Another interesting aspect of DPK can be found in reported solid state structures of metal–DPK (1:2) complexes [1–3]. These structures show that one of the oxygen atoms from the newly formed diol on the ligand also interacts with the metal atom, thereby making the ligand tridentate in character rather than bidentate. Moreover, as illustrated in Fig. 2 the coordinated oxygen group lies in an off-axial position and this M–O bond makes an angle with the line normal to the equatorial plane such that in 1:2 metal to DPK complexes the metal cation possesses a distorted octahedral *trans* N_4O_2 coordination sphere [3].

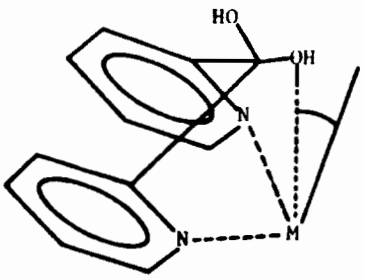

Fig. 2. DPK hydrate–metal bonding.

*Author to whom correspondence should be addressed.

0020-1693/90/$3.50

There have been reports of the UV–Vis spectral behavior of DPK with various metal cations under a variety of conditions [1, 4, 5]. Although much has been done with aqueous DPK systems, there has been no report of observations of the UV–Vis spectrum of a metal cation with DPK in aqueous solution over time. The spectral evidence suggests that final complex formation is slow in aqueous solution requiring days or weeks to complete depending on the metal ion. We also report two new metal: DPK hydrate solid state structures, each displaying some distortion within the octahedral coordination sphere.

UV–Vis Spectroscopy

Copper(II) was selected for this study because extensive solution work has been reported [6–8] and also because the molecular structure of (1:2) in the solid state is known [3]. Chromium(III) was selected because there has been no report of it forming complexes with DPK under any conditions.

Aqueous solutions of $Cu(NO_3)_2$ and $CrCl_3$ with DPK were studied spectrophotometrically under a variety of conditions. The spectra were recorded on a Perkin-Elmer 330 UV–Vis spectrophotometer. Figure 3 illustrates the initial shift of the absorption peak for Cu(II) towards higher energy upon the addition of DPK in a 1:2 metal ion/ligand ratio. A rapid darkening of the combined solution accompanied this spectral movement. Comparison of the spectral shifts observed when ethylenediamine (en), bipyridylamine (bpyamine) and bipyridyl (bpy), are added to aqueous metal ion solutions indicates that the coordination is through the two nitrogen atoms on the ligand in all cases.

An interesting and previously unreported phenomenon was observed first in the spectrum of Cu(II): DPK solution after a period of five weeks (Fig. 3).

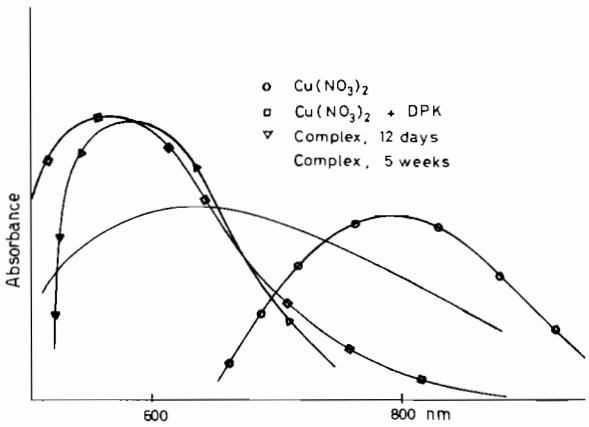

Fig. 3. UV–Vis spectra: $Cu(NO_3)_2$ + DPK, 1 to 2 ratio; total movement over time.

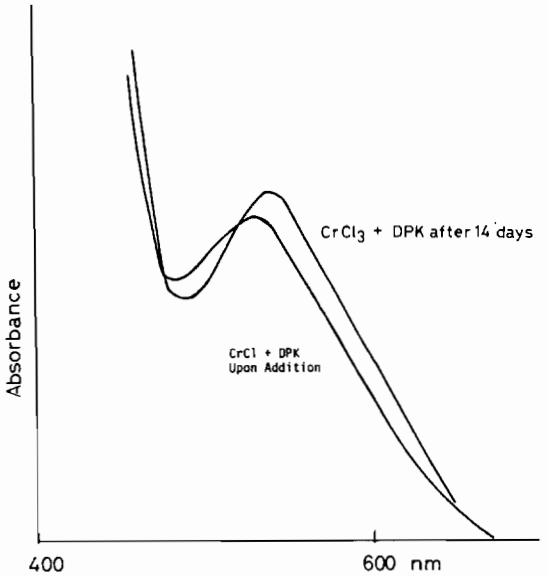

Fig. 4. UV–Vis spectra: $CrCl_3$ + DPK, 1 to 2 ratio; reverse movement.

Not only does the absorption peak broaden out but it also shifts back toward lower energy. Upon closer investigation it was found that indeed a reverse movement of the peak began within one week of the metal ion–DPK combination in solution.

Chromium(III) spectra were recorded in parallel with those of Cu(II). Changes in the Cr(III)–DPK solution spectra were much slower. Upon the addition of DPK to the Cr(III) solution, the color slowly changed from green to red over a period of 25 min. Figure 4 shows the final position of the Cr(III)–DPK absorption peak and the reverse shift toward lower energy is seen. However this movement was not as pronounced as that for the Cu(II)–DPK system. Spectra were also recorded for Cr(III) with en, dpyamine and bpy and results parallel those for the copper system, i.e. equal shifts toward higher energy of the absorption peak for all ligands as occurs initially with DPK.

The pH of each of these aqueous solutions was also determined as the UV–Vis spectra were being recorded, using a Chemtrix type 40E pH meter along with a magnetic stirrer. The pH meter was standardized with commercial pH 4 and pH 10 buffers. The pH of these solutions becomes more acidic with time (3.2 for the copper system and 2.0 for the chromium system).

UV–Vis spectra were again taken of the respective solutions to see if any absorption peak shift occurred after the pH was modified by addition of strong relatively non-ligating acids or bases. Figures 5 and 6 show that there was indeed movement of the absorption peak with a change in solution pH.

The absorption spectrum of the Cu:DPK system is shown at pH 4 in Fig. 6. The position of the peak

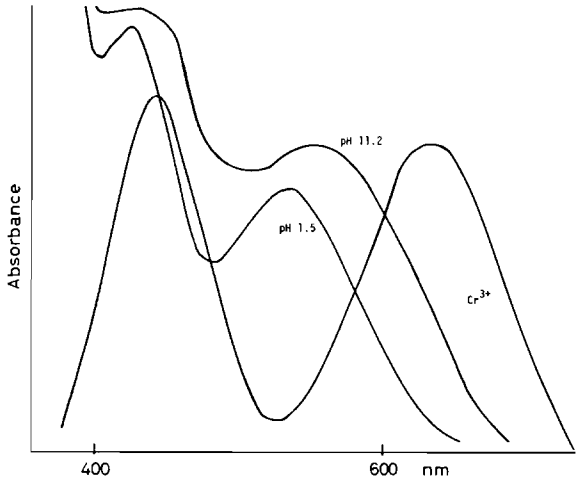

Fig. 5. Absorption spectra: Cr:DPK 1:2 ratio.

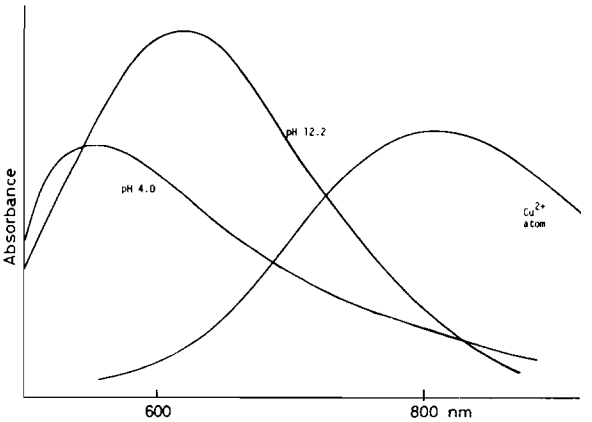

Fig. 6. Absorption spectra: Cu:DPK 1:2 ratio.

upon addition of DPK to Cu(II) is shown as well as the absorption peak after addition of 6 N NaOH (pH = 12.2) and 6 N HNO_3 (pH = 4). For the Cr(III): DPK system 6 N HCl was used and gave similar results.

X-ray Analysis

Data Collection

Crystals suitable for X-ray single crystal structure analysis were obtained by allowing the aqueous solvent to slowly evaporate from solutions of $CrCl_3 \cdot 6H_2O$ and $RuCl_3 \cdot 3H_2O$, respectively, which con-

TABLE 1. Crystal data for $[Cr(C_{11}H_8N_2(OH)(O))_2]Cl \cdot 4H_2O$ (I) and $[Ru(C_{11}H_8N_2(OH)(O))_2] \cdot 8H_2O$ (II)

	I	II
Empirical formula	$CrC_{22}H_{26}N_4O_8Cl$	$RuC_{22}H_{34}N_4O_{12}$
Formula weight	561.9	647.6
Crystal class	monoclinic	triclinic
Space group	$C2/c$	$P\bar{1}$
Extinction conditions	hkl $h + k = 2n$ $h0l$ $l = 2n$ ($h = 2n$) $0k0$ $k = 2n$	none
a (Å)	11.19(1)	9.829(9)
b (Å)	14.67(1)	8.829(9)
c (Å)	17.12(1)	8.908(7)
α (°)	90.0	99.79(6)
β (°)	104.06(1)	103.04(6)
γ (°)	90.0	76.30(7)
V (Å^3)	2731	714
Z	4	1
μ (cm^{-1}) (Mo Kα)	5.66	5.95
ρ_c (g/cm)	1.37	1.42
Diffractometer	Datex	Syntex $P2_1$
Monochromator	graphite crystal	
Radiation, Mo Kα	$\lambda = 0.71098$	$\lambda = 0.71034$
Scan type	ω-scan	ω-scan
Standard reflections	3 (measured every 75 reflections)	1 (measured every 100 reflections)
Octants collected	$hkl, -h - kl$	$hkl, -hkl, h - kl, -h - kl$
Reflections collected	3150	2719
Max 2θ (°)	50	50
Min 2θ (°)	3	3
No. unique reflections ($I_{obs} > 3\sigma I_I$	1848	2406
No. parameters refined	179	193
R[a]	0.086	0.050
R_w[a]	0.117	0.066

[a] $R = [\Sigma(||F_o| - |F_c||)^2/\Sigma F_o^2]^{1/2}$; $R_w = [\Sigma w(||F_o| - |F_c||)^2/\Sigma w F_o^2]^{1/2}$; $w = 1/\sigma F^2$.

tained metal ion to DPK in a 1:2 ratio. The resulting crystals were rectangular in shape with approximate dimensions of 0.18 X 0.19 X 0.38 mm for the Cr(III) complex and 0.10 X 0.12 X 0.11 mm for the Ru complex. The crystals were attached to glass fibers and mounted on standard X, Y, Z translation goniometer heads. All intensity data were collected at ambient temperature. The unit cell parameters were initially calculated using the automatic indexing procedure BLIND [9]. The space groups $C2/c$ for the Cr(III) complex and $P\bar{1}$ for the Ru complex were consistent with the systematic absences observed in the data. Statistical analyses indicated both structures were centrosymmetric. Table 1 contains a tabulation of the pertinent information relevant to data collection.

TABLE 2. Positional parameters of the non-hydrogen atoms $\times 10^4$

Atom	x	y	z
I			
Cr	0	0	0
N1	863(4)	296(4)	1179(3)
C1	886(7)	1060(5)	1596(4)
C2	1549(8)	1113(6)	2385(4)
C3	2187(8)	369(6)	2756(4)
C4	2135(7)	−445(6)	2329(4)
C5	1455(6)	−439(4)	1527(4)
C11	1231(6)	−1271(4)	955(4)
O1	1246(4)	−947(3)	196(2)
O2	2106(4)	−1949(4)	1249(3)
N2	−912(4)	−992(4)	475(3)
C21	−2114(7)	−1110(5)	424(4)
C22	−2527(8)	−1828(6)	820(5)
C23	−1661(8)	−2414(6)	1280(5)
C24	−422(8)	−2295(5)	1338(4)
C25	−83(7)	−1574(4)	933(4)
C1	53(4)	4906(3)	602(3)
O3	1854(5)	6525(4)	423(3)
O4	−262(6)	3233(4)	1661(4)
O5	4637(19)	62(10)	1233(9)
O6	5000	959(10)	2500
II			
Ru	0	0	0
N1	328(5)	1878(4)	1319(5)
C1	−652(7)	3156(6)	1294(8)
C2	−186(8)	4314(6)	2269(9)
C3	1310(8)	4156(6)	3238(9)
C4	2313(7)	2831(6)	3248(7)
C5	1789(6)	1725(5)	2269(6)
C11	2698(6)	199(6)	2123(6)
O1	2382(4)	−324(6)	532(4)
O2	4334(4)	50(4)	2753(4)
N2	454(5)	−795(4)	2094(5)
C21	−443(7)	−1463(6)	2630(7)
C22	105(8)	−1968(6)	4077(7)
C23	1574(8)	−1774(6)	4947(7)
C24	2504(7)	−1070(6)	4381(7)
C25	1904(6)	−603(5)	2940(6)
O3	3748(6)	4202(5)	386(5)
O4	5751(6)	1570(5)	1568(6)
O5	6275(6)	7321(6)	2731(8)
O6	5478(12)	5034(10)	3683(9)

Structure and Refinement

For each structure, the metal atom position was obtained by analysis of the three-dimensional Patterson map. The remaining non-hydrogen atoms were located from subsequent electron density maps [10]. These positions and the associated anisotropic thermal parameters were refined first by using block diagonal least-squares calculations [9]. The final

TABLE 3. Intramolecular bond distances (Å)

Atoms	Distance
I	
Cr–O1	1.939(5)
Cr–N1	2.061(5)
Cr–N2	2.055(6)
N1–C1	1.326(10)
N1–O5	1.328(10)
C1–C2	1.376(11)
C2–C3	1.373(13)
C3–C4	1.394(13)
C4–C5	1.389(10)
C5–C11	1.547(10)
C11–O2	1.401(9)
C11–O1	1.387(8)
C11–C25	1.528(11)
N2–C21	1.338(9)
N2–C25	1.360(9)
C21–C22	1.391(13)
C22–C23	1.388(14)
C23–C24	1.377(13)
C24–C25	1.368(10)
II	
Ru–O1	1.975(4)
Ru–N1	2.057(4)
Ru–N2	2.065(5)
N1–C1	1.340(7)
N1–C5	1.347(7)
C1–C2	1.391(9)
C2–C3	1.378(10)
C3–C4	1.386(8)
C4–C5	1.372(8)
C5–C11	1.519(7)
C11–O2	1.387(6)
C11–O1	1.411(6)
C11–C25	1.519(7)
N2–C21	1.335(7)
N2–C25	1.351(7)
C21–C22	1.401(9)
C22–C23	1.372(9)
C23–C24	1.396(9)
C24–C25	1.384(8)

TABLE 4. Intramolecular bond angles (°)

Atoms	Angle	Atoms	angle
I		II	
N1–Cr–N2	94.52(21)	N1–Ru–N2	94.42(17)
N1–C4–O1	99.51(19)	N1–Ru–O1	101.02(17)
N2–Cr–O1	99.82(21)	N2–Ru–O1	78.89(17)
Cr–N1–C1	130.43(48)	Ru–N1–C1	129.31(38)
Cr–N1–C5	109.41(44)	Ru–N1–C5	111.04(31)
N1–C1–C2	120.75(75)	N1–C1–C2	120.44(55)
C1–C2–C3	120.37(80)	C1–C2–C3	119.93(55)
C2–C3–C4	119.20(69)	C2–C3–C4	119.00(57)
C3–C4–C5	116.68(73)	C3–C4–C5	118.63(55)
C4–C5–N1	122.62(67)	C4–C5–N1	122.39(46)
N1–C5–C11	111.76(57)	N1–C5–C11	111.10(42)
Cr–N2–C21	130.85(52)	Ru–N2–C21	129.07(37)
Cr–N2–C25	109.73(45)	Ru–N2–C25	110.65(33)
C21–N2–C25	119.36(63)	C21–N2–C25	120.24(46)
N2–C21–C22	120.93(77)	N2–C21–C22	120.47(53)
C21–C22–C23	118.50(86)	C21–C22–C23	119.69(56)
C22–C23–C24	120.92(81)	C22–C23–C24	119.55(56)
C23–C24–C25	117.35(73)	C23–C24–C25	118.13(53)
C24–C25–N2	122.93(71)	C24–C25–N2	121.91(47)
C5–C11–C25	104.62(58)	C5–C11–C25	106.62(41)
C5–C11–O1	106.56(56)	C5–C11–O1	106.62(42)
C5–C11–O2	110.01(57)	C5–C11–O2	112.81(44)
C25–C11–O1	107.82(55)	C25–C11–O1	106.40(42)
C25–C11–O2	112.80(59)	C25–C11–O2	110.78(43)
O1–C11–O2	114.41(57)	O1–C11–O2	113.17(40)

TABLE 5. Thermal parameters of the non-hydrogen atoms × 10^4

Atom	B_{11}	B_{12}	B_{33}	B_{12}	B_{13}	B_{23}
I						
Cr	49(1)	29(1)	21(1)	−1(1)	5(1)	3(1)
N1	56(5)	32(3)	24(2)	−8(3)	8(3)	−6(2)
C1	79(7)	46(4)	34(3)	−13(4)	20(4)	−8(3)
C2	106(9)	54(5)	37(3)	−12(6)	20(5)	−19(3)
C3	98(8)	67(5)	26(3)	−22(5)	6(4)	−8(3)
C4	73(7)	56(5)	33(3)	−7(5)	6(4)	−8(3)
C5	69(6)	36(3)	27(2)	0(4)	11(3)	2(3)
C11	70(6)	36(3)	25(2)	−7(4)	4(3)	−1(2)
O1	66(4)	38(2)	25(2)	5(2)	11(2)	−3(2)
O2	72(5)	42(3)	37(2)	9(3)	0(2)	6(2)
N2	60(5)	35(3)	32(2)	−3(3)	12(3)	−4(2)
C21	76(7)	46(4)	40(3)	−11(5)	19(4)	−9(3)
C22	103(9)	62(6)	47(4)	−33(6)	32(5)	−16(4)
C23	115(9)	51(5)	41(4)	−24(6)	19(5)	3(3)
C24	112(9)	43(4)	32(3)	−14(5)	11(4)	6(3)
C25	82(7)	34(4)	28(3)	−2(4)	9(4)	−2(3)
C1	94(4)	62(3)	48(2)	−20(3)	8(2)	4(2)
O3	118(6)	53(3)	53(3)	−8(4)	34(3)	−10(3)
O4	112(7)	73(4)	57(3)	10(4)	5(4)	7(3)
O5	310(31)	73(9)	60(8)	−40(13)	18(12)	−4(7)
II						
Ru	74(1)	70(1)	74(1)	−18(1)	14(1)	7(1)
N1	89(6)	68(5)	92(6)	−16(5)	17(1)	5(5)

(continued)

TABLE 5. *(continued)*

Atom	B_{11}	B_{12}	B_{33}	B_{12}	B_{13}	B_{23}
C1	131(10)	86(7)	142(10)	−13(7)	15(8)	6(7)
C2	182(12)	69(7)	205(13)	−13(7)	29(10)	2(8)
C3	186(12)	92(8)	183(12)	−43(8)	16(10)	−15(8)
C4	142(10)	107(8)	105(9)	−52(7)	18(8)	−6(7)
C5	96(8)	78(6)	88(8)	−29(6)	11(6)	5(6)
C11	83(8)	92(6)	78(7)	−26(6)	2(6)	11(6)
O1	71(5)	92(4)	82(5)	−20(4)	12(4)	6(4)
O2	77(5)	125(5)	110(6)	−26(4)	−9(5)	15(5)
N2	106(7)	70(5)	80(6)	−20(5)	20(5)	11(5)
C21	126(9)	81(6)	116(9)	−28(6)	49(7)	8(6)
C22	187(12)	93(7)	120(9)	−33(7)	60(9)	20(7)
C23	199(13)	105(8)	105(9)	−18(8)	39(9)	32(7)
C24	133(10)	95(7)	104(9)	−10(7)	8(8)	18(6)
C25	99(8)	72(6)	88(8)	−22(6)	16(6)	9(6)
O3	297(11)	123(6)	117(7)	46(6)	48(7)	43(6)
O4	186(9)	188(8)	157(8)	−41(6)	78(7)	6(6)
O5	197(10)	176(8)	330(14)	−47(7)	5(10)	66(9)
O6	685(30)	458(20)	254(15)	−359(21)	8(17)	110(15)

TABLE 6. Positional parameters of the hydrogen atoms $\times 10^4$

Atom	x	y	z
I			
H1	404	1637	1314
H2	1578	1713	2712
H3	2700	388	3356
H4	2620	−1019	2613
H5	−2759	−657	76
H6	−3470	−1918	775
H7	−1943	−2962	1584
H8	220	−2744	1687
II			
H1	−1830	3289	532
H2	−993	5354	2248
H3	1694	5061	3987
H4	3496	4693	4011
H5	−1612	−1615	1950
H6	−622	−2513	4513
H7	2030	−2166	6061
H8	3680	−924	5060

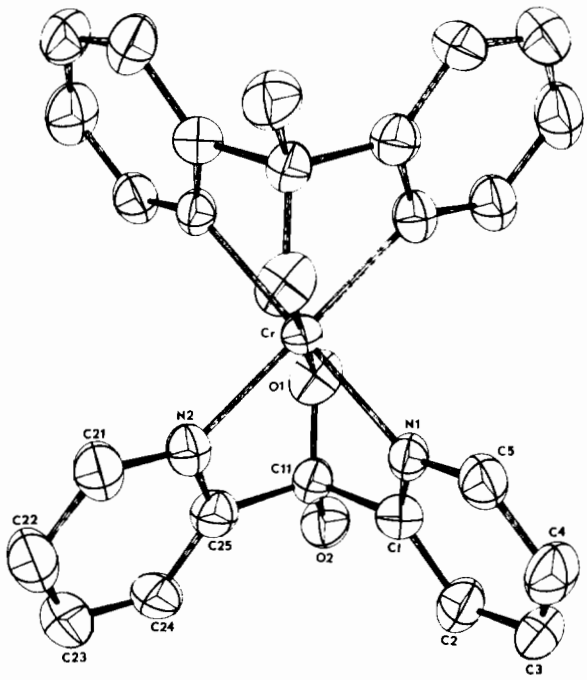

Fig. 7. ORTEP representation of I.

refinement was done using full matrix least-squares techniques. Positions for hydrogen atoms were calculated assuming a C–H distance of 1.05 Å. Final positional parameters for the atoms in the two structures are listed in Table 2, interatomic distances in Table 3 and interatomic angles in Table 4. Thermal parameters of the non-hydrogen atoms and positional parameters of the hydrogen atoms are given in Tables 5 and 6, respectively. Figures 7 an 8 are ORTEP [11] drawings of the Cr:DPK and Ru:DPK structures respectively. Because the metal atoms occupy sites of high symmetry refinements were attempted in both the appropriate centric and acentric space groups. In each case the choice of the centrosymmetric group was confirmed by the fact that subsequent refinement steps converged to more chemically realistic models using that symmetry.

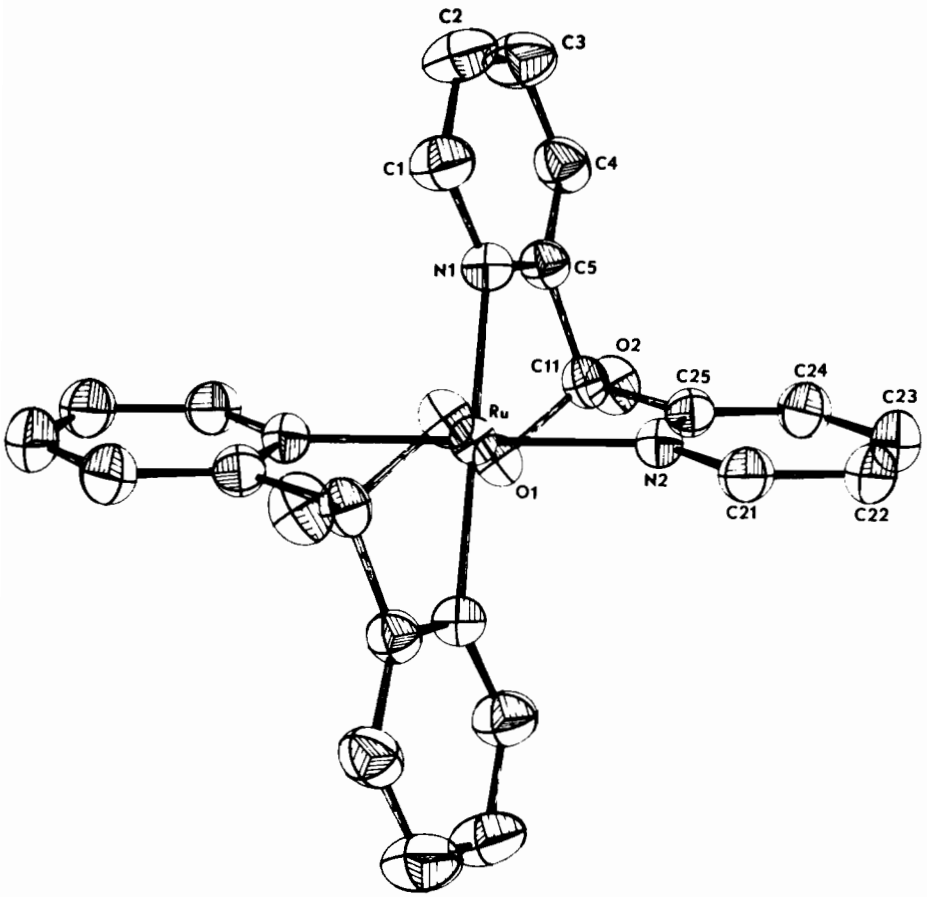

Fig. 8. ORTEP representation of II.

Discussion

UV–Vis Spectra

The reverse shift towards lower energy observed subsequent to the initial peak shift to higher energy was found to be unique to DPK systems. The solutions containing either Cu(II) or Cr(III) with en, bpyamine and bpy showed only the initial shift towards higher energy with no reverse shift back towards lower energy over time. It is interesting to note that these reverse shifts were not accompanied by a detectable rise in the pH of the system. As noted earlier, the respective spectra for the Cu(II): DPK and Cr(III):DPK systems appear to be cyclic in the sense that the absorption peak could be shifted by the addition of acid or base. The reverse shift observed over time however does not appear to be due to a fluctuation in pH, since the solutions remained acidic as indicated.

The Structures

The ORTEP drawings of both the Cr(III) and Ru complexes show the two DPK ligands bonded to the metal cation in a tridentate fashion. The geometry about the metal ion can be described as a distorted octahedron due to the unusual off-axis coordination of the oxygen atom. In these two aspects, both structures are quite similar to previously reported 1:2 complexes [3].

In the Ru complex, the metal–ligand bond distances are very similar (Ru–N ave. = 2.061 Å, Ru–O = 1.975 Å) which indicates similar bond strength within the coordination sphere. The off-axis angle formed between the Ru–O bond and the line normal to the equatorial plane was found to be approximately 15°.

For the Cr(III) complex, the metal–ligand bond distances are also similar (Cr–N ave. = 2.058 Å, Cr–O 1.941 Å). The off-axis angle formed between the Cr–O bond and the line normal to the equatorial plane was found to be approximately 12°. This is the smallest off-axis angle yet reported, possibly due to the high octahedral field stabilization energy in d^3 complexes.

The bond distances and angles in the DPK hydrate ligands are normal in both structures. The average C–C bond distances of the ring atoms are 1.383 and 1.385 Å for the Cr(III) and Ru structures, re-

spectively which are quite close to the accepted value for pyridine of 1.395(1) Å [12]. Likewise the average C–N bond distances, 1.339 and 1.343 Å are very close to the accepted value of 1.340(1) Å; the average bond angles within the rings are 120.0° in both cases. Hence, there is no apparent strain or distortion within the pyrdine rings.

The charge on the chromium complex may be discussed in several different ways. Analogy with structures such as the M(DPY hydrate)$_2^{2+}$ where M = Cu(II) or Ni(II) [3] would provide a model whereby the ketone hydrate apparently has two uncharged OH groups on the carbon atom (one of which is bonded to the metal atom). The complex has a 2+ charge with appropriate counter ions to neutralize this charge ($2Cl^-$ or $2NO_3^-$ in the case of the Cu(II) complexes or SO_4^{2-} in the case of the nickel complex). The chromium complex would then require two OH^- counter ions in addition to the one (disordered) chloride ion. This model presumes that a hydroxide compound is precipitated from acidic solutions (~ pH 2–3). A more plausible model would be one in which the oxygen atoms bonded to the chromium ion have lost their proton. The complex has, with this assumption, a +1 charge. This charge is neutralized by the chloride ion. The chemical analysis for I is consistent with this model. Calc. for $CrC_{22}H_{26}N_4O_8Cl$: C, 47.0; H, 4.7; N, 10.0; Cl, 6.3. Found: C, 47.1; H, 4.6; N, 10.1; Cl, 6.4%. We believe the latter model is more reasonable.

The ruthenium complex, **II**, may be described in several ways also. Here we favor the choice of a complex where the ruthenium atom is in the II oxidation state. The complex is thus uncharged and the additional oxygen atoms located on Fourier maps are from water molecules of hydration. A Ru(III) complex would require one or more hydroxide ions as counter ions which we believe to be unlikely. Ru(II) complexes have been prepared from $RuCl_3 \cdot 3H_2O$ and DPK [13]. Conductivity studies would not necessarily establish the charge on the complex in solution. We have NMR evidence that indicates that several DPK complex species exist in aqueous solution at any time leading up to precipitation using aluminum or lead ions [14]. It is interesting to note that the intra-ligand pyridyl ring dihedral angles are 101° for the Cr(III) complex and 109° for the Ru(II) complex as compared to 180° expected for a planar

TABLE 7. Bond parameters in 1:2 complexes

Compound	Dihedral angle (°)	Δ[a] (Å)	Bite (Å)
[Cu(DPKhydrate)$_2$]Cl$_2$	115	0.47	2.774
[Cu(DPKhydrate)$_2$](NO$_3$)$_2$	113	0.45	2.782
[Ni(DPKhydrate)$_2$]SO$_4$	117	0.02	2.962
[Ru(DPKhydrate)$_2$]	109	−0.09	2.792
[Cr(DPKhydrate)$_2$]Cl	101	−0.12	2.537

[a]Δ = difference between $(M-O)_{axial}$ and $(M-N)_{equatorial}$ lengths. Other structures of DPK hydrate and 2,2,-bis(2-pyridyl)-1,3-dioxolane, diox, coordinated to transition metal ions have been reported. A symmary of these compounds and the structures discussed above (Table 7) provide a rough correlation of off-axis bonding as a function of crystal field stabilization energy, CFSE (Table 8).

TABLE 8. DPK hydrate and diox complexes

Metal ion	Reference	Off-axis angle	No. of electrons	CFSE[a]		ΔCFSE
				Octahedral	Square planar	Square planar – Octahedral
Au^{3+}	1	31.28	d^8	−12*Dq*	−24.6*Dq*	−12.6*Dq*
Pd^{2+}	1	29.4	d^8	−12	−24.6	−12.6
Cu^{2+} (diox)	15	28.31	d^9	−6	−12.3	−6.3
Ni^{2+} (diox)	15	24.9	d^8	−12	−24.6	−12.6
Cu^{2+}	3	22.6	d^9	−6	−12.3	−6.3
Cu^{2+}	3	21.5	d^9	−6	−12.3	−6.3
Cu^{2+} (diox)	15	19.2	d^9	−6	−12.3	−6.3
Au^{3+}	2	18.3	d^8	−12	−24.6	−12.3
Ru^{2+}	this work	15.0	d^4	−12	−11.3	−0.7
Cr^{3+}	this work	12.5	d^3	−12	−15.4	−3.4

[a]The crystal field stabilization energies are taken form ref. 16. Strong field splitting is assumed where appropriate (Ru^{2+} was included as weak field). Jahn–Teller distortions have not been considered.

DPK ligand. These are quite significant deviations from planarity for the DPK ligand. Upon examination of the data in Table 7, it is evident that the deviation of the pyridyl rings from co-planarity appears to be completed with strong M–O coordination although a number of other factors probably also have a role. Table 7 summarizes five 1:2 metal to DPK structures reported (this work and three structures previously reported, see ref. 3). These data show an approximate correlation between off-axis angle and square planar site preference. Other effects such as steric ones are also likely to be important and may account for the deviation shown by the second gold complex.

Conclusions

The two structures are in good agreement with others reported to date. UV–Vis spectra have been shown to aid in the investigation of the progress of coordination about the transition metal cation. After accounting for the respective movements of the absorption peak due to the initial coordination of the four nitrogen atoms (1:2 metal/DPK ratio) initially, the reverse shift appears to be related to the coordination of the hydroxyl groups in the 'off-axial position'. A shift toward lower energy would result because the ligated oxygen group replaces the water molecule already in the axial position on the metal, due to solvation, and the former is lower in the spectrochemical series. This coupled with the fact that the coordination is not exactly in the axial position but rather off-axis, as evidenced by the solid state structures, likely leads to a lowering in the average ligand field strength of the transition metal cation, consequently resulting in a movement of the absorption peak toward lower energy.

Acknowledgement

This work was supported in part by the U.S. Department of Energy, Office of Basic Energy Sciences, Materials Sciences Division, under contract W-7405-Eng-82.

References

1 G. Annibale, L. Canovese, L. Cattalini, G. Natile, M. Biagini-Cingi, A. Manotti-Lanfredi and A. Tiripecchio, *J. Chem. Soc., Dalton Trans.*, (1981) 2280.
2 P. K. Byers, A. J. Canty, L. M. Engelhardt, J. M. Patric, and A. H. White, *J. Chem. Soc., Dalton Trans.*, (1985) 981.
3 S. L. Wang, J. W. Richardson, S. J. Briggs, R. A. Jacobson and W. P. Jensen, *Inorg. Chim. Acta, 111* (1986) 67.
4 J. D. Ortego, D. D. Waters and C. S. Steele, *J. Inorg. Nucl. Chem., 36* (1974) 751.
5 B. E. Fischer and H. Sigel, *J. Inorg. Nucl. Chem., 37* (1975) 2127.
6 R. R. Osborne and W. R. McWhinnie, *J. Chem. Soc. A*, (1968) 2153.
7 M. C. Feller and R. Robson, *Aust. J. Chem., 21* (1968) 2919.
8 M. C. Feller and R. Robson, *Aust. J. Chem., 23* (1970) 1997.
9 R. A. Jacobson, *J. Appl. Crystallogr., 9* (1976) 115.
10 D. R. Powell and R. A. Jacobson, *FOUR*, general crystallography program, *Rep. IS-4737*, U.S. Department of Energy, 1980.
11 C. K. Johnson, *ORTEP-II*, A FORTRAN thermal ellipsoid plot program for crystal structure illustrations, U.S. AEC *Report ORNL-3794* (second revision with supplemental instructions), 1971.
12 *Tables of Interatomic Distances and Configurations in Molecules and Ions*, The Chemical Society, London, 1958.
13 A. Basu, T. G. Kasar and N. Y. Sapre, *Inorg. Chem., 27* (1988) 4539.
14 W. P. Jensen and C. Boever, unpublished work.
15 G. R. Newkome, H. C. R. Taylor, F. R. Fronczek and V. K. Gupta, *Inorg. Chem., 25* (1986) 1149.
16 J. E. Huheey, *Inorganic Chemistry*, Harper and Row, New York, 1983, p. 412.